Intermolecular Interactions, Nucleation, and Thermodynamics of Crystallization of Hemoglobin C

Peter G. Vekilov,* Angela R. Feeling-Taylor,†¶ Dimiter N. Petsev,*† Oleg Galkin,* Ronald L. Nagel,‡§ and Rhoda Elison Hirsch‡¶

*Department of Chemical Engineering, University of Houston, Houston, Texas 77204; †Center for Microgravity and Materials Research, University of Alabama in Huntsville, Huntsville, Alabama 35899; the Departments of ‡Medicine (Division of Hematology), §Physiology and Biophysics, and ¶Anatomy and Structural Biology, Albert Einstein College of Medicine and Montefiore Hospital, Comprehensive Sickle Cell Center, The Bronx, New York 10461 USA

ABSTRACT The mutated hemoglobin HbC (β6 Glu→Lys), in the oxygenated (R) liganded state, forms crystals inside red blood cells of patients with CC and SC diseases. Static and dynamic light scattering characterization of the interactions between the R-state (CO) HbC, HbA, and HbS molecules in low-ionic-strength solutions showed that electrostatics is unimportant and that the interactions are dominated by the specific binding of solutions' ions to the proteins. Microscopic observations and determinations of the nucleation statistics showed that the crystals of HbC nucleate and grow by the attachment of native molecules from the solution and that concurrent amorphous phases, spherulites, and microfibers are not building blocks for the crystal. Using a novel miniaturized light-scintillation technique, we quantified a strong retrograde solubility dependence on temperature. Thermodynamic analyses of HbC crystallization yielded a high positive enthalpy of 155 kJ mol^{-1}, i.e., the specific interactions favor HbC molecules in the solute state. Then, HbC crystallization is only possible because of the huge entropy gain of 610 J mol^{-1} K^{-1}, likely stemming from the release of up to 10 water molecules per protein intermolecular contact—hydrophobic interaction. Thus, the higher crystallization propensity of R-state HbC is attributable to increased hydrophobicity resulting from the conformational changes that accompany the HbC β6 mutation.

INTRODUCTION

Hemoglobin (Hb) C is a mutated Hb that, when oxygenated, forms crystals inside red blood cells of patients with the homozygous CC disease (Hirsch et al., 1985; Lawrence et al., 1991). The Hb C molecule differs from the most common variant, Hb A, by a single mutation at the sixth amino acid position of the β subunit that replaces the negatively charged glutamic acid with a positively charged lysine (β^6 Glu→Lys) (Hunt and Ingram, 1958). The intraerythrocytic crystals contribute to the clinical pathogenesis of the disease (Lessin et al., 1969). Oxy-HbC crystals also form in red cells of patients doubly heterozygous for both HbS and HbC, i.e., who have the SC disease, a severe, life-threatening condition (Nagel and Lawrence, 1991). Thus, insight into the thermodynamics and kinetics of HbC crystallization, in particular at the molecular level, is relevant to the understanding of the pathogenesis of the CC and SC diseases. Furthermore, this is a model system for numerous other "condensation diseases," in which the pathology is related to the formation of a condensed phase (crystals, polymers, plaques, aggregates, etc.) of proteins: sickle cell anemia (Eaton and Hofrichter, 1990), the eye cataract (Benedek et al., 1999), Alzheimer's (Lomakin et al., 1996), and possibly the prion diseases (Koo et al., 1999). Crystallization dynamics studies with Hb C also contribute to efforts to determine the relationship between the mutation, structural changes, and the propensity for formation of solid phases. Last, while the structure of deoxy-HbC has been determined (Fitzgerald and Love, 1979), there have been no published reports to date detailing the structure of liganded or R-state Hb C at resolution sufficient for the visualization of the structural changes evidenced by the spectroscopic approaches (Hirsch et al., 1996).

In previous work, in situ observations of crystal growth in osmotically dehydrated red blood cells were interpreted in terms of a pathway involving formation of small "paracrystals," followed by their alignment into tetragonal and hexagonal crystals (Charache et al., 1967). The suggested mechanism of alignment of the microribbons is similar to the one implied for the other β^6 Hb variant, deoxy HbS (Bluemke et al., 1988; Lessin et al., 1969; Makinen and Sigountos, 1984; Potel et al., 1984). This pathway is at odds with the crystallization mechanism established for a broad variety of proteins under a broad range of conditions (McPherson et al., 2000; Yau et al., 2000a; Yau et al., 2000b; Yau and Vekilov, 2000): in all cases crystals nucleate by the association of single molecules into a critical cluster, the nucleus, and grow by the attachment of single molecules to this nucleus. Thus, data on the statistics of crystal nucleation and real-time, in situ monitoring of the elementary acts of molecular attachment to the crystals are needed to decide, if indeed, hemoglobin crystallization follows a pathway distinct from the one of most other proteins.

Several studies of mutated hemoglobins have shown that even single amino acid substitutions, at least at the β^6 site, cause local conformational changes, especially in the proximal region (Fronticelli, 1978; Fronticelli and Gold, 1976;

Submitted February 13, 2002, and accepted for publication May 1, 2002.

Address reprint requests to Peter G. Vekilov, Department of Chemical Engineering, Engineering Building I, University of Houston, Houston, TX 77204-4004. Tel.: 713-743-4315; Fax: 713-743-4323; E-mail: vekilov@uh.edu.

0006-3495/02/08/1147/10 $2.00

Fung and Ho, 1975; Fung et al., 1975), that can be communicated distally to promote additional structural change (Perutz, 1976). Recent front-face fluorescence, ultraviolet resonance spectroscopy and visible resonance Raman spectroscopy suggest that the A helix, the secondary structural region where the mutation resides, appears locally displaced so that the hydrogen bond between β^{15} Trp and β^{72} Ser is weakened (Hirsch et al., 1996). It has been suggested that this structural change may promote association and assembly of Hb C molecules into ordered, e.g., crystalline, structures (Hirsch et al., 1996). Concurrently, the analyses of the thermodynamics of crystallization, presented below, suggest the participation of molecular regions away from the mutation site in the aggregation process.

Another issue is linked to the factors underlying the unique propensity of HbC to form crystals in vivo. It has been the subject of an intense discussion, and the propensity has often been attributed solely to the charge difference between this protein and the other β6 mutants. The results presented below suggest that the structuring of the water molecules around the Hb molecule, dependent on the hydrophobicity of the Hb molecule, may be an overwhelming factor.

Thus, the issues addressed in this paper are: 1) What are the components of the thermodynamics driving force for the formation of the HbC crystals? We search for answers in the data on the temperature dependence of the solubility. 2) Are the interactions between the molecules in the solutions prior to crystallization solely determined by the electrostatic charge or by other factors? We study the interactions by a combination of static and dynamic light scattering. 3) Do HbC crystals nucleate by the association of single HbC molecules, or are other solid phases, such as amorphous precipitate, "ribbons," "spherulites," etc., involved? To address this issue, we look at the nucleation statistics.

The crystallization studies reported here were carried out at in potassium phosphate buffer at concentrations between 1.5 and 2.0 M, at pH 7.37. Our attempts to carry out crystallization studies at the low buffer concentrations yielded crystals with phosphate in the range of 0.6–1.6 M only if polyethylene glycol is added; at even lower phosphate concentrations no crystallization of CO-HbC occurs; other authors have reported deoxy-HbC crystals at lower phosphate concentrations in the presence of PEG (Fitzgerald and Love, 1979). The interactions and thermodynamics in protein-water-polymer systems are completely different from a system that does not contain the polymer (O. Galkin and P. G. Vekilov, unpublished). We did not consider results obtained with PEG relevant to the goals of this investigation. Since high electrolyte concentrations screen the charges and mask the effects of the charge differences between the Hb mutants, to access the importance of the electrostatic interactions in the formation of condensed phases of the hemoglobin mutants, we used a combined static and dynamic light scattering technique at a buffer concentration of 0.05 M, with two buffers, phosphate and HEPES, alone and in combination with 0.05 to 0.25 M NaCl.

Because of the higher stability of CO-HbC as compared to oxy-HbC, the CO form is often used in studies of the R-state HbC. This was the form employed in this study.

MATERIALS AND METHODS

HbC solutions

The procedures used to obtain HbC from blood donated by a CC patient are discussed by (Hirsch et al., 2001). For the crystallization studies, 20 mg ml^{-1} CO-HbC solutions in 1.9 M KH_2PO_4/K_2HPO_4 at pH 7.37 were prepared. Due to the lower solubility of HbC at lower temperatures, the crystallizing solution was cooled to 4°C to dissolve nuclei that may have formed during the handling of the materials. For the light scattering studies, HbC stock solution was dialyzed at 4°C against the appropriate buffer and salt solution.

Static and dynamic light scattering determinations

The dynamic light scattering measurements were performed on a Brookhaven 200 SM goniometer with a HeNe laser (Spectra Physics 127/V, 35 mV), operating at 632.8 nm wavelength. The small size and isotropic shape of the hemoglobin molecules precludes any significant angular dependence of the scattered light, in agreement with a previous result (Hall et al., 1980). Hence, all determinations were performed at a scattering angle of 90°, for further experimental details, see Petsev et al. (2000, 2001).

Dynamic light scattering (DLS) measures the diffusion coefficient of the sample, which can be related to the molecular size of spherical particles using the Stokes-Einstein expression (Schmitz, 1990)

$$D = \frac{kT}{3\pi\eta d_h}, \tag{1}$$

where d_h is the hydrodynamic diameter of the molecule, η is the solvent viscosity and k_BT is the thermal energy. Estimates of the average particle size and size distributions were obtained form the DLS data and Eq. 1 using the CONTIN algorithm (Provencher 1979, 1982a,b).

The static light scattering experiments were performed on the same equipment. The refractive index increment (dn/dC) necessary to interpret that data was measured using an Optilab (Wyatt Technologies) differential refractometer operating at the wavelength of the laser, 632.8 nm. Static light scattering is based on determinations of the concentration dependence of the scattered light intensity. The reciprocal intensity or Rayleigh ratio R_θ is plotted as a function of the protein concentration C in g ml^{-1}, the so-called Debye plot (Zimm, 1948)

$$\frac{KC}{R_\theta} = \frac{1}{M_w}(1 + 2A_2M_wC), \tag{2}$$

where M_w is the molecular mass of the protein, and $K = 1/N_A(2\pi n_0/\lambda^2)^2(dn/dC)^2$ is a constant, N_A is Avogadro's number, λ is the wavelength, n_0 is the refractive index of the solvent, and dn/dC_p is the refractive index

increment. The quantity A_2 in Eq. 2 is the second osmotic virial coefficient in ml mol g^{-2} units. It is convenient to write it in dimensionless form

$$B_2 = \frac{3A_2M_w^2}{4\pi N_A d_h^3}. \quad (3)$$

Solubility measurements

The existing methods for determination of the solubility of Hb and its $\beta 6$ variants (Adachi and Asakura, 1981; Charache et al., 1967; Itano, 1953), based on probing the Hb concentration after crystallization has ceased, have produced divergent results, with the variability attributed to unfinished crystallization, i.e., to data taken before equilibrium between crystals and solution has been reached (Adachi and Asakura, 1981). Hence, we designed a novel scintillation method (Feeling-Taylor et al., 1999), in which the correspondence between temperature and equilibrium concentration is established by dissolving crystals. This approach provides twofold advantages over methods in which the equilibrium is approached from the growth side: 1) during dissolution, layers start retracting from the crystal's edges, and thus no "dissolution layer source" is needed. 2) Impurity pinning of steps (Cabrera and Vermileya, 1958; Voronkov and Rashkovich, 1994) is believed to be less common during layer retraction. Kinetic hindrances, associated with growth layer generation and with impurity effects at low supersaturations, can lead to growth cessation in supersaturated solutions, and thus bias equilibrium point determinations from the supersaturated side. The experimental setup, a miniaturized scintillation technique for protein solubility determinations, and procedures employed in this work are discussed in detail (Feeling-Taylor et al., 1999).

Determination of the nucleation statistics

Existing experimental methods for determinations of nucleation statistics and the derived homogeneous nucleation rates (Bartell and Dibble, 1991; Hung et al., 1989) are not applicable or would produce ambiguous results for protein systems. Even protein-specific methods, such as the techniques that use levitating droplets (Arnold et al., 1999; Izmailov et al., 1999), are prone to evaporation of solution from the liquid-air interface. Light scattering (Kam, 1978; Malkin and McPherson, 1994), although a powerful technique, is heavily dependent on assumptions about the interactions between the molecules for data interpretation. Hence, a novel technique for direct determinations of nucleation statistics was used.

To begin a run, the CO-HbC solution is loaded at a temperature chosen to prevent crystallization or other phase transitions. Since solubility has a retrograde dependence on temperature, then the temperature is raised to a selected T_1 at which nucleation occurs. After a time Δt_1 temperature is lowered from the nucleation temperature T_1 to the growth temperature T_2. At T_2, supersaturation is at levels where nucleation rate is practically zero, but the crystals already formed can grow to detectable dimensions (Tammann, 1922). This allows separation of the nucleation from the ensuing growth. After the growth stage, the crystals nucleated at T_1 during Δt_1 are counted (Galkin and Vekilov, 1999).

To obtain reproducible statistical characteristics of the random nucleation process, 100 (or 400 in later versions of the setup) simultaneous trials take place under identical conditions, in solution droplets of volume 0.7 μl. To suppress the undesired nucleation at the solution air interface, the droplets were suspended in inert silicone oil, used in optimizations of the crystallization conditions of a variety of proteins (Chayen, 1999). To extract the nucleation rate from the time dependence of the number of nucleated crystals, five droplet arrays are subjected to the nucleation supersaturation at increasing time intervals Δt_1. These Δt_1's ranged from 12 min to 8 h. Thus, the determination of one nucleation rate data point is based upon statistics over 2000 protein solution droplets. The experimental procedures are described in detail by Galkin and Vekilov (1999).

In all experiments discussed here, T_1 was between 24 and 30°C, T_2 was 12°C, the concentration of CO-HbC was between 15 and 20 mg ml^{-1}.

RESULTS

Determination of size distributions and the second virial coefficients

To characterize the interactions between the proteins in the R-state form, we carried out a combined static and dynamic light scattering investigation of CO saturated solutions Hb A, S, and C in 0.05 M phosphate and HEPES (*N*-[2-hydroxyethyl]piperazine-N′-[4-ethanesulphonic]) buffers. At concentrations of the hemoglobin lower than about 5 mg ml^{-1}, the dimer-tetramer equilibrium is shifted in favor of $\alpha\beta$ dimers (Herskovits et al., 1977). Since the goal of the studies reported here is to investigate the interaction between whole hemoglobin units, we only worked at concentrations above 5 or 6 mg ml^{-1}, at which dissociation is undetectable (Berreta et al., 1997; Elbaum et al., 1976; Lunelli et al., 1993). The highest protein concentrations were <30 mg ml^{-1}.

Determinations of the species size distributions were carried out using dynamic light scattering with samples of Hb A, S, and C. A typical monodisperse size distribution is shown Fig. 1 *a*. The data in Fig. 1 *A* and other identical distributions revealed that throughout the concentration range 5–30 mg ml^{-1}, the solutions contained a single protein species of a size between 5 and 6 nm, in agreement with the 5.5 nm known for hemoglobin from crystallographic determinations (Perutz, 1969; Vasquez et al., 1998). The narrow range of sizes in Fig. 1 *A* and the single peak centered on the expected value certify that the light scattering signal is produced by native molecules of the respective Hb species.

A typical static light scattering data plot in the coordinates of Eq. 2 is shown in Fig. 1 *B*. From the slope of the straight line, we extract the second osmotic virial coefficient in its dimensional form, A_2, and its dimensionless form, B_2. Since the dynamic light scattering results indicate that neither dissociation into $\alpha\beta$ dimers nor aggregation occur in our samples, we conclude that the variations of A_2 with the chemical composition of the solution are fully attributable to changes in the intermolecular interactions.

Fig. 2 shows the dependencies of the virial coefficients A_2 for hemoglobins A, C, and S, as a function of the concentration of NaCl at pH 7.35 maintained by 0.05 mol of either phosphate or HEPES buffers. In all cases, the values of A_2 are strongly positive, and the value of A_2 in HEPES is 4.2×10^{-4} ml mol g^{-2} for all $C_{NaCl} \leq 0.2$ M.

Solubility of CO-HbC as a function of temperature

In the studies of the temperature dependence of the solubility of CO-HbC, the hemoglobin concentration was 8.0–35.0

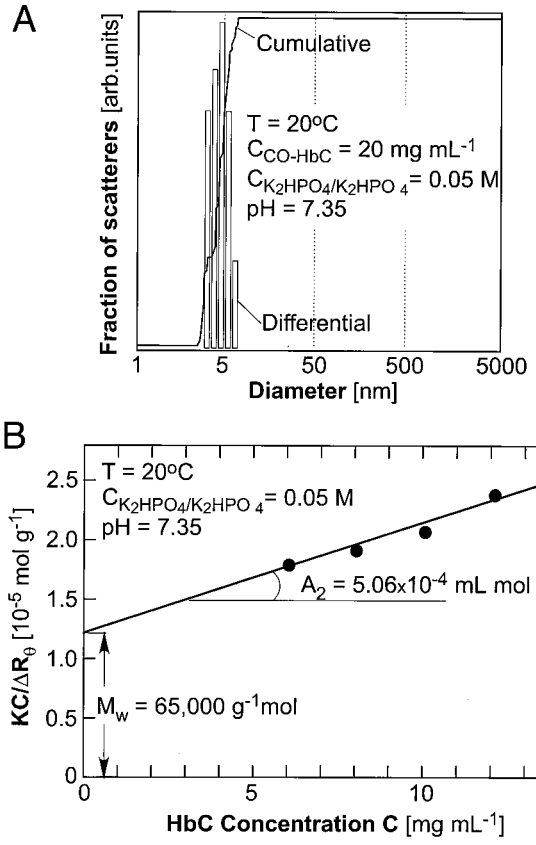

FIGURE 1 Typical static and dynamic light scattering data. Shown in this figure are data obtained for COHbC. The same technique was applied to COHbA and COHbS (data not shown). (*A*) Size distribution of CO-HbC molecules deduced from dynamic light scattering data using CONTIN at (*B*) Debye plot—dependence of the reciprocal Raleigh ratio ΔR_θ on the concentration of CO-HbC *C*. The conditions of the determinations are listed in the plots.

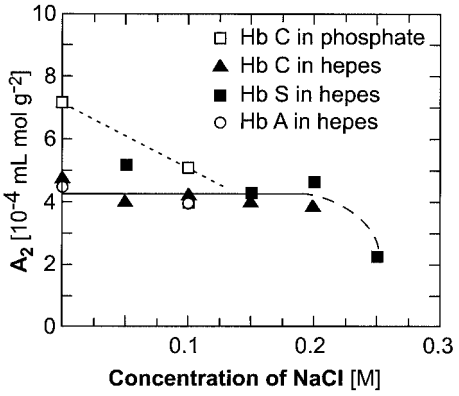

FIGURE 2 Dependence of the second osmotic virial coefficient A_2 for the CO-HbC, CO-HbS, and CO-HbA as a function of the concentration of NaCl in 0.05 M phosphate and 0.05 M HEPES buffers. Solid, dotted, and dashed lines are just guides for the eye.

mg ml^{-1} and the concentration of the KH_2PO_4/K_2HPO_4 buffer was 1.4–2.0 M, at pH 7.37. Preliminary investigations had indicated an extreme sensitivity of the CO-HbC solubility to minor variations in the buffer concentration. Hence, to ensure reproducibility of the results, we prepared 20 l KH_2PO_4/K_2HPO_4 buffer at 2.0 M. Half of it was diluted to 1.9 M and aliquots were taken for all studies at this buffer concentration presented in Fig. 3. Aliquots from the remaining half were diluted to the required concentration and used to obtain the results presented in Fig. 4.

The solubility determination procedures discussed above allowed determinations of the temperatures at which a CO-HbC solution of a certain composition is in equilibrium with the CO-HbC crystals. An experimental run to determine a solubility point took between 6 and 24 hs. The integrity of CO-HbC throughout the experiment was preserved: tests post-experiment showed VIS spectra consistent with CO-Hb and the absence of met-Hb. Temperatures and CO-HbC concentrations at equilibrium for fixed buffer concentration of 1.9 M and pH 7.37 are plotted in Fig. 3. The higher solubility at lower temperature, i.e., "retrograde temperature dependence of solubility" (Rosenberger et al., 1993), is similar to the one known for deoxy-HbS (Ross et al., 1977), and has been encountered with other proteins.

Fig. 4 shows the dependence of the equilibrium temperature for a solution containing 20 mg ml^{-1} CO-HbC on the phosphate concentration. We see that higher buffer concentrations strongly reduce CO-HbC solubility, a "salting-out" behavior. One way to evaluate the efficacy of buffer concentration changes on the solubility is to compare the changes in T_{eq} induced by a variation of the precipitant concentration in Fig. 4, to the variation T_{eq} due to changing Hb concentration in Fig. 3. We see that a 10% variation in the buffer concentration is equivalent to a temperature change that induces a sevenfold change in solubility, in

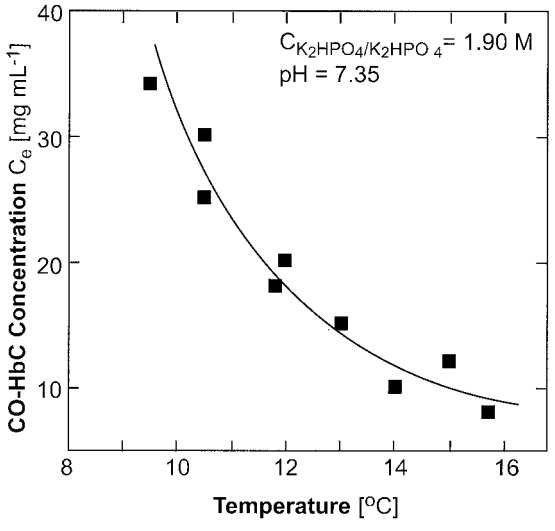

FIGURE 3 Dependence of solubility C_e of carbomonoxy-hemoglobin C on temperature at conditions indicated in the plot. Points are experimental results; curve is fit to Eq. 1 using ΔH = 155 kJ/mol.

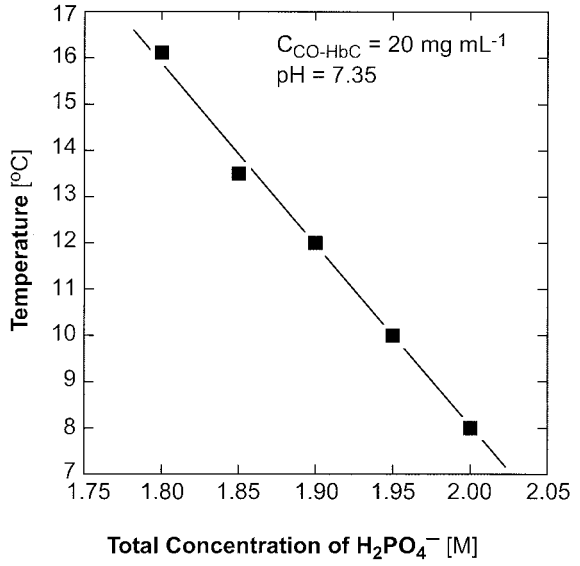

FIGURE 4 Dependence of the equilibrium temperature of a 20 mg ml^{-1} CO-HbC solution on phosphate buffer concentration at pH 7.35.

quantitative agreement with previous results for Hb A (Adachi and Asakura, 1981).

Microscopic observations and statistics of nucleation

The microscopic observations were carried out after ~12–14 h at a lower supersaturation level allowing the growth of crystals nucleated during Δt_1. Hence, most of the crystals had grown until all CO-HbC material had been recruited into crystals as noted by the near complete lack of color. All of the formed crystals had the typical tetragonal bipyramid habit, see Fig. 5 *B*. The droplets that did not contain crystals had uniform bright red color, shown as gray in Fig. 5 *C*. Spectroscopic analyses of the solutions revealed that the CO-HbC was intact and no conversion to met-Hb had occurred.

In some of the experiments at elevated supersaturations, stemming from high temperature and/or high CO-HbC concentration, a few of the droplets contained spherulitic domains, Fig. 5 *D*. Judging from its color (the human eye is sensitive to a 0.1 unit change in optical density), the solution surrounding such domains has significantly higher concentration of Hb than the solution in contact with crystals of similar, or even much smaller size. Hence, the amount of HbC per unit volume of the spherulites is much lower than in the crystals, and we conclude that they are amorphous formations with loose structure. Furthermore, as Fig. 5 *D* shows, the solution in contact with the spherulitic domains contains a high number of linear objects of a few tens of micrometers in length. These likely are the microribbons seen before in CO-HbC solution under identical conditions (Hirsch et al., 2001). These microribbons were never seen in the droplets that only contain crystals.

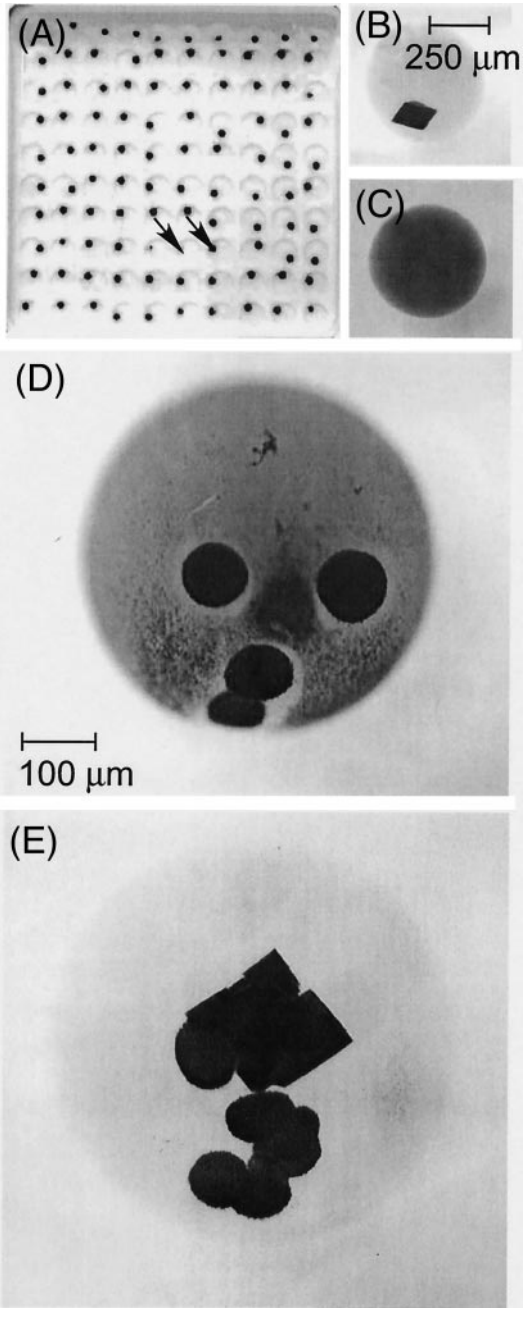

FIGURE 5 Microscopic observation of the formation of solid phases and determination of nucleation statistics. (*A*) an array of 100 droplets of CO-HbC solution sunk in silicate oil. In later test, arrays of 400 droplets were used. Arrows point at droplets shown in *b* and *c*. (*B*) A droplet containing a crystal. Note the pale solution color, indicative of nearly complete depletion of the HbC in the solution. (*C*) A droplet without any sold phase. (*D*) A droplet from an array different than the one in *a* showing the two amorphous phases: round spherulitic aggregates and the microribbons. Note the solution color is significantly denser than in *b*. (*E*) A droplet with spherulites and crystals that appeared several hours after the spherulites. Crystal formation leads to dissolution of the microribbons.

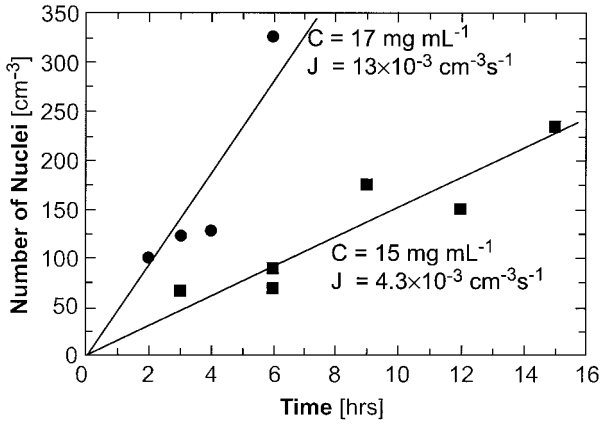

FIGURE 6 Time-dependence of nucleation at 30°C. The CO-HbC concentration is indicated in the plot. The homogeneous nucleation rate *J*, calculated from the slopes of the straight lines, is shown.

In a few droplets containing spherulites, crystals appeared 2–3 h after spherulite formation (Fig. 5 *E*). Eventually, the microribbons disappeared in these droplets. These observations do not indicate 1) transformation of the spherulites into crystals, or 2) incorporation of the microribbons by the crystals: for (1) we note the huge difference in molecular density between crystals and spherulites; for (2), we note that the diffusive mobility of the loose-structured microribbons should be very low, and it is unlikely that they move from the droplet periphery to the crystal and become incorporated in it. Hence, the spherulites and microribbons participate in the crystallization process only as heterogeneous nucleation centers and a sources of CO-HbC material upon their dissolution.

We compared the overall nucleation statistics to a scenario whereby all crystals nucleate and grow by the attachment of single molecules. The distribution of the number of crystals in the droplets in an array was always Poissonian, exactly as seen for crystals of the protein lysozyme (Galkin and Vekilov, 1999, 2000). Furthermore, the rate of nucleation *J*, defined as the number of crystals that nucleate in a unit volume per unit time, is a very strong function of the CO-HbC concentration (Fig. 6).

DISCUSSION

Specificity of interactions between hemoglobin molecules

Interactions and non-ideality in hemoglobin solutions, in particular HbS, have been studied by osmometry (Adair, 1928; Prouty et al., 1985), sedimentation (Williams, 1973), as well as by light scattering techniques (Elbaum et al., 1976; Kam and Hofrichter, 1986). Since in the sequence HbA, S, and C, the charge at the $\beta 6$ site changes from negative to neutral to positive, it has been speculated that this one elementary unit charge difference underlies, through electrostatic intermolecular interactions, the variability of the solid phases formed by these three variants. On the other hand, the deviations from ideality found by osmometry and sedimentation were solely attributed to the finite volume of the hemoglobin molecules, the so-called hard-sphere model (Minton, 1977; Ross et al., 1978).

According to Eq. 3, the value of the virial coefficient A_2 determined above corresponds to a value of the dimensionless $B_2 = 16$, fourfold higher than the value for non-interacting hard spheres of $B_2 = 4$. This is higher than the values of B_2 for HbS of 4–6 stemming from earlier work (Minton, 1977; Ross and Minton, 1977a,b). Note that the discrepancy is not attributable to limiting the current analysis to B_2 and neglecting B_3, B_4, etc.; it was shown that at Hb concentrations <40 mg ml^{-1}, the contribution of the higher order virial coefficients is insignificant (Ross and Minton, 1977a). The high B_2 values indicate strong repulsion between the Hb molecules, incompatible with a model of non-interacting hard spheres.

Furthermore, the repulsion between the Hb molecules in HEPES is not affected by the addition of NaCl; B_2 is constant in certain [NaCl] range, and despite the charge differences, the virial coefficients of the three Hb mutants are practically identical. We conclude that the observed repulsion is not of electrostatic origin. We attribute this weakness of the electrostatic forces to the chosen pH being very close to the isoelectric points for these Hb mutants, leading to small molecular charges, <5 (Antonini and Brunori, 1971). On the other hand, the different A_2 and B_2 values in phosphate and HEPES buffers, suggest that the strong intermolecular repulsion for all Hb mutants are due to the specific interaction with the NaCl ions and the ions into which the buffers dissociate.

Mechanisms of nucleation of HbC crystals

The microscopic observations and nucleation statistics, discussed above, show that two HbC amorphous phases, the spherulites and the microribbons are not building blocks of the crystal. Furthermore, the Poissonian distribution of the frequency of the nucleation events and the strong, exponential dependencies of the nucleation rate on supersaturation are typical for nucleation pathways involving single molecules attachment (Mutaftschiev, 1993). We conclude that nucleation of CO-HbC crystals occurs through the association of single molecules and is identical to nucleation of deoxy-HbS polymers (Ferrone et al., 1985a,b; Hofrichter, 1986).

Thermodynamics of HbC crystallization

The transition from protein solute to protein crystals has been likened to gas-solid condensation. Upon reaching a threshold density, gas molecules form a new phase; as the

protein molecules in an aqueous solution reach their threshold concentration, the solubility, a crystal forms (Oasawa and Kasi, 1962). In both systems, the thermodynamics of the phase transitions are based on the cumulative net effects of enthalpic and entropic contribution. However, there is a very important difference between the two systems. While the entropy effect of the gas-to-solid transition is limited to the entropy loss upon the immobilization of the molecules in the crystal, the entropy balance of the protein solution-to-solid phase transition has two components. Besides the similar entropy loss of the protein molecules upon incorporation into the crystal, the solution-to-solid phase transition may also include an entropy gain due to the release of the significantly higher number of water molecules associated with the proteins in the solution prior to crystallization (Kuntz and Zipp, 1977; Lauffer, 1975; Tanford, 1961; Zipp et al., 1977).

The retrograde temperature dependence of solubility (Fig. 3) can be understood in terms of the Gibbs-Helmholtz equation (Eisenberg and Crothers, 1979).

$$\left(\frac{\partial \ln K_{\text{cryst}}}{\partial T}\right)_{\text{p}} = -\left[\frac{\partial(\Delta G^{\circ}/\text{R}T)}{\partial T}\right]_{\text{p}} = \frac{\Delta H^{\circ}}{\text{R}T^2}, \qquad (4)$$

where K_{cryst} is the equilibrium constant for crystallization, T is the absolute temperature, ΔG° is the standard change of Gibbs free energy upon crystallization, $\text{R} = 8.314$ J mol^{-1} K^{-1} is the universal gas constant, and ΔH° is the standard crystallization enthalpy.

The crystallization equilibrium constant K_{cryst} can be represented as (Atkins 1998)

$$K_{\text{cryst}} = a_{\text{e}}^{-1} = \left(\gamma_{\text{e}}\frac{C_{\text{e}}}{C^{\circ}}\right)^{-1} \approx \left(\frac{C_{\text{e}}}{C^{\circ}}\right)^{-1}, \qquad (5)$$

where a_{e} is the activity of the Hb in solution in equilibrium with the crystals, γ_{e} and C_{e} are, respectively, the corresponding activity coefficient and concentration, and $C^{\circ} = 1$ mol kg^{-1} is the concentration of the solution in its standard state. The last approximate equality in Eq. 5 is based on the assumption that $\gamma_{\text{e}} \approx 1$, i.e., the solution is close to ideal. To avoid this assumption, we could experimentally evaluate γ at the crystallizing conditions by using its link to the second virial coefficient (Hill, 1963), as done before the apoferritin crystallization (Yau et al., 2000a). Unfortunately, as discussed above, because of the shifts of the average particle size, indicative of protein aggregation, such determinations are not possible for a crystallizing solution of CO-HbC. For an indication of the error introduced by the ideality assumption, we compare it with the deviation from ideality of the osmotic pressure of a solution of deoxy-HbS: at $C = 20$ mg ml^{-1} it is 5%, and 7% at $C = 40$ mg ml^{-1} (Ross and Minton, 1977a). We conclude that the ideality assumption may bring about at most 10% error in the following evaluations.

Combining Eqs. 4 and 5, we get

$$\left[\frac{\partial \ln(C_{\text{e}}/C^{\circ})}{\partial T}\right]_{\text{p}} = -\frac{\Delta H^{\circ}}{\text{R}T^2}. \qquad (6)$$

The data in Fig. 3 fit a single exponent with a best-fit value of $\Delta H^{\circ} = 155 \pm 10$ kJ mol^{-1}, with the positive sign of the enthalpy stemming from the negative sign of $(\partial C_{\text{e}}/\partial T)$. Positive crystallization enthalpy, i.e., endothermic crystallization, means that heat is consumed during crystallization. For the process to be thermodynamically permissible, the free energy of crystallization at constant pressure,

$$\Delta G^{\circ} = \Delta H^{\circ} - T\Delta S^{\circ}, \qquad (7)$$

must be negative, i.e., the entropy component $T\Delta S^{\circ} > \Delta H^{\circ}$.

Eq. 5 and the data in Fig. 3 can help us evaluate ΔG°. Using that $K_{\text{cryst}} = \exp(\Delta \text{G}^{\circ}/RT)$,

$$\Delta G^{\circ} = RT \ln a_{\text{e}} \cong RT \ln(C_{\text{e}}/C^{\circ}). \qquad (8)$$

At $T = 16°C$, with $C_{\text{e}} = 9$ mg ml^{-1} $= 0.00014$ mol kg^{-1} and $\Delta G^{\circ} = -21.3$ kJ mol^{-1}. At $T = 10°$C, with $C_{\text{e}} = 32$ mg ml^{-1} $= 0.0005$ mol kg^{-1} we get $\Delta G^{\circ} = -17.9$ kJ mol^{-1}. From these and ΔH°, using Eq. 7, we get for both temperatures $\Delta S^{\circ} = 610$ J mol^{-1} K^{-1}. Note that both ΔH° and ΔS° do not change in the above temperature interval, and all changes in ΔG° are accounted for by the T factor in Eq. 7.

The sign and the magnitude of the entropy change indicate that the crystallization of hemoglobin C is accompanied by the release of solvent molecules attached to the Hb molecules in solution, and where the number of the released molecules is high. Since water is the dominant component of the solvent, we can safely assume that the main contribution to the crystallization entropy is its release. Intermolecular attraction of large molecules, that arises when the structured water around hydrophobic patches at the surface becomes disordered as molecules are brought closer, has been called "hydrophobic force" (Tanford, 1980). From our data on hemoglobin, we cannot judge if the water molecules are adjacent to hydrophilic of hydrophobic surface patches. However, in experiments with another protein, apoferritin, it was found that water structuring around hydrophilic patches leads to effective repulsion (Petsev et al., 2000; Petsev and Vekilov, 2000). Hence, we assume that the above entropy gain, i.e., the free energy component that drives the molecules into the crystal, is the hydrophobic interaction between the protein molecules (Israelachvili and Wennerstrom, 1996; Israelachvili, 1995; Tanford, 1980).

This conclusion allows us to crudely estimate the number of water molecules n_{w} released at the contact between two hemoglobin molecules. We can tentatively divide the entropy effect ΔS° between $\Delta S^{\circ}_{\text{protein}}$ and $\Delta S^{\circ}_{\text{solvent}}$,

$$\Delta S^{\circ} = \Delta S^{\circ}_{\text{protein}} + \Delta S^{\circ}_{\text{solvent}}, \qquad (9)$$

with, likely, $\Delta S^{\circ}_{\text{protein}} < 0$ and $\Delta S^{\circ}_{\text{solvent}} \gg 0$. One way to do this is by assuming $\Delta S^{\circ}_{\text{protein}}$ is insignificant. Such assump-

tion may be justified if the contribution of the new vibrational degrees of freedom created upon the incorporation of a molecule, $\Delta S_{vibr} > 0$, is comparable in magnitude to the translational and rotational entropies of the free molecule in solution, lost upon incorporation, $\Delta S_{trans} + \Delta S_{rot} < 0$ (Tidor and Karplus, 1994). Then, $\Delta S^{\circ}_{water} \approx 600$ J mol^{-1} K^{-1}. On the other hand, if we rely on the published estimates for entropy loss of single protein molecules of ~ -120 J mol^{-1} K^{-1} (Fersht, 1999; Finkelstein and Janin, 1989), $\Delta S^{\circ}_{solvent} \approx$ 700 J mol^{-1} K^{-1}.

Following an analogy first put forth by Tanford (1980), we compare the entropy effect of Hb crystallization to the entropy change for melting of ice, at 273 K, $\Delta S^{\circ}_{ice} = 22$ J mol^{-1} K^{-1} (Dunitz, 1994; Eisenberg and Crothers, 1979; Eisenberg and Kauzmann, 1969). Similarly, estimates of the entropy loss due to the tying up of hydration water in crystals have yielded 25–29 J mol^{-1} K^{-1} (Dunitz, 1994). Using these numbers, the above values of ΔS°_{water} reflect the release of ~20–30 water molecules. With six molecules as nearest neighbors in the tetragonal crystal lattice (Perutz, 1969; Vasquez et al., 1998) and three intermolecular bonds per molecule in the crystal, this corresponds to the release of $n_w \approx 7$–10 water molecules per intermolecular bond.

How does this compare to findings for other protein crystals? The standard free energy of formation of a single intermolecular bond in apoferritin crystals is -7.9 kJ mol^{-1} (Yau et al., 2000b); and, since $\Delta H^{\circ} \cong 0$ (Petsev and others 2001), is fully attributable to the entropy gain due to the release of solvent (Yau et al., 2000a), i.e., $\Delta S^{\circ}_{solvent} = 26.6$ J mol^{-1} K^{-1}. Comparing this to ΔS°_{ice}, this corresponds to $n_w \approx 2$ for apoferritin.

With HbC, the release of ten water molecules leads to an entropy gain that overcomes the contribution of the unfavorable enthalpy to the free energy by only $\Delta G^{\circ}/\Delta H^{\circ} \approx 20/155 \approx 13\%$. We can define a critical n_w^{crit}, for which the entropy contribution to the free energy is equal to the enthalpy loss. Then, with

$$\Delta S^{\circ} = (Z/2) n_w^{crit} \Delta S^{\circ}_{ice} \quad (10)$$

(Z being the coordination number in the crystal, in a primitive tetragonal lattice $Z = 6$), the condition

$$\Delta H^{\circ} = T\Delta S^{\circ} \quad (11)$$

stemming from Eq. 7 with $\Delta G^{\circ} = 0$, yields at $T = 293$ K $n_w^{crit} \approx 8$ for HbC.

The hydrophobic interactions are enhanced by electrolytes in concentrations of the order of a few molar (Tanford, 1980) and this may underlie the need for a high phosphate concentration in the crystallization of HbC in vitro. An important consequence of this conclusion is that the crystallization of HbC in the low-electrolyte environment in the red cell cytosol must be facilitated by another attractive interaction. Likely candidates include specific and nonspecific interactions involving the polymer and organic molecules present in % concentrations in the red cell cytosol (Pennell, 1974).

Judged only from the amino-acid composition, hemoglobin A has about the same hydrophobicity as HbC. On the other hand, the fact that the crystallization of HbA in vitro requires even higher concentrations of phosphate suggests lower hydrophobicity. This contradiction indicates that the conformational changes that occur as consequences of the single amino acid substitution render the HbC molecule more hydrophobic than the HbA (Hirsch et al., 1996). Following the same line of thought, the more hydrophobic HbS, in which the charged glutamic acid residue is replaced by the non-polar valine, crystallizes even at 0.1–0.2 M phosphate.

This work was supported by NHLBI, NIH through Grants RO1 HL58038, RO1HL5824, and Graduate Scholarship S531HL09563 to A.R.F.-T; the Office of Biological and Physical Research, NASA, through Grants NAG8-1354 and NAG8-1857; American Heart Association, Heritage Affiliate, Grant-in-Aid 9950989T; Universities Space Research Association Research Contract 03537.000.013; and the State of Alabama thorough the Center for Microgravity and Materials Research at the University of Alabama in Huntsville.

REFERENCES

Adachi, K., and T. Asakura. 1981. Aggregation and crystallization of hemoglobins A, S, and C: probable formation of different nuclei for gelation and crystallization. *J. Biol. Chem.* 256:1824–1830.

Adair, G. S. 1928. A theory of partial osmotic pressures and membrane equilibria with special reference to the application of Dalton's law to hemoglobin solutions in the presence of salts. *Proc. Roy. Soc. London A.* 120:573–603.

Antonini, E., and M. Brunori. 1971. Hemoglobin and Mioglobin in Their Reactions with Ligands. North Holland, Amsterdam.

Arnold, S., N. L. Goddard, and N. Wotherspoon. 1999. Convertible electrodynamic levitator trap to quasielectrostatic levitator for microparticle nucleation studies. *Rev. Sci. Instr.* 70:1473–1477.

Atkins, P. 1998. Physical Chemistry. W. H. Freeman, New York.

Bartell, L. S., and T. S. Dibble. 1991. Electron diffraction studies of the kinetics of phase changes in molecular clusters: freezing of CCl_4 in supersonic flow. *J. Phys. Chem.* 95:1159–1167.

Benedek, G. B., J. Pande, G. M. Thurston, and J. I. Clark. 1999. Theoretical and experimental basis for the inhibition of cataract. *Prog. Retin. Eye Res.* 18:391–402.

Berreta, S., G. Chirico, D. Arosio, and G. Baldini. 1997. Photon correlation spectroscopy of interacting and dissociating hemoglobin. *J. Chem. Phys.* 106:8427–8435.

Bluemke, D. A., B. Carragher, M. J. Potel, and R. Josephs. 1988. Structural analysis of polymers of sickle cell hemoglobin. II. Sickle hemoglobin macrofibers. *J. Mol. Biol.* 199:333–348.

Cabrera, N., and D. A. Vermileya. 1958. The growth of crystals form solution. *In* Growth and Perfection of Crystals (Doremus, R. H., Roberts, B. W., Turnbul, D., editors). Wiley, New York.

Charache, S., C. L. Conley, D. F. Waugh, R. J. Ugoretz, and J. R. Spurrell. 1967. Pathogenesis of hemolytic anemia in homozygous hemoglobin C disease. *J. Clin. Invest.* 46:1795–811.

Chayen, N. E. 1999. Crystallization with oils: a new dimention in macromolecular crystal growth. *J. Crystal Growth.* 196:434–441.

Dunitz, J. D. 1994. The entropic cost of bound water in crystals and biomolecules. *Nature* 264:670–670.

Eaton, W. A., and J. Hofrichter. 1990. Sickle cell hemoglobin polimerization. *In* Advances in Protein Chemistry (Anfinsen, C. B., Edsal, J. T., Richards, F. M., Eisenberg, D. S., editors) Academic Press, San Diego, 63–279.

Eisenberg, D., and D. Crothers. 1979. Physical Chemistry with Applications to Life Sciences. The Benjamin/Cummins, Menlo Park, CA.

Eisenberg, D., and W. Kauzmann. 1969. The Structure and Properties of Water. Oxford University Press, Oxford.

Elbaum, D., R. L. Nagel, and T. T. Herskovitz. 1976. Aggregation of deoxyhemoglobin S at low concentrations. *J. Biol. Chem.* 251: 7657–7660.

Feeling-Taylor, A. R., R. M. Banish, R. E. Hirsch, and P. G. Vekilov. 1999. Miniaturized scintillation technique for protein solubility determinations. *Rev. Sci. Instr.* 70:2845–2849.

Ferrone, F. A., H. Hofrichter, and W. A. Eaton. 1985a. Kinetics of sickle cell hemoglobin polymerization. I. Studies using temperature jump and laser photolysis techniques. *J. Mol. Biol.* 183:591–610.

Ferrone, F. A., H. Hofrichter, and W. A. Eaton. 1985b. Kinetics of sickle cell hemoglobin polymerization. II. A double nucleation mechanism. *J. Mol. Biol.* 183:611–631.

Fersht, A. 1999. Structure and Mechanism in Protein Science. W. H. Freeman, New York.

Finkelstein, A., and J. Janin. 1989. The price of lost freedom: entropy of bimolecular complex formation. *Protein Eng.* 3:1–10.

Fitzgerald, P. M., and W. E. Love. 1979. Structure of deoxy hemoglobin C (β6Glu replaced by Lys) in two crystal forms. *J. Mol. Biol.* 132: 603–619.

Fronticelli, C. 1978. Effect of the beta6 Glu replaced by Val mutation on the optical activity of hemoglobin S and of its β subunits. *J. Biol. Chem.* 253:2288–2291.

Fronticelli, C., and R. Gold. 1976. Conformational relevance of the β6Glu replaced by Val mutation in the β subunits and in the β(1–55) and β(1–30) peptides of hemoglobin S. *J. Biol. Chem.* 251:4968–4972.

Fung, L. W., and C. Ho. 1975. A proton nuclear magnetic resonance study of the quaternary structure of human homoglobins in water. *Biochemistry.* 14:2526–2535.

Fung, L. W., K. L. Lin, and C. Ho. 1975. High-resolution proton nuclear magnetic resonance studies of sickle cell hemoglobin. *Biochemistry.* 14:3424–3430.

Galkin, O., and P. G. Vekilov. 1999. Direct determination of the nucleation rate of protein crystals. *J. Phys. Chem.* 103:10965–10971.

Galkin, O., and P. G. Vekilov. 2000. Are nucleation kinetics of protein crystals similar to those of liquid droplets? *J. Am. Chem. Soc.* 122: 156–163.

Hall, R. S., Y. S. Oh, and C. S. Johnson. 1980. Photon correlation spectroscopy in strongly adsorbing and concentrated samples with applications to unliganded hemoglobin. *J. Phys. Chem.* 84:756–767.

Herskovits, T. T., S. M. Cavanagh, and R. C. San George. 1977. Light-scattering investigations of the subunit dissociation of human hemoglobin A: effects of various neutral salts. *Biochemistry.* 16:5795–5801.

Hill, T. L. 1963. Thermodynamics of Small Systems. Benjamin, New York.

Hirsch, R. E., M. J. Lin, G. J. Vidugiris, S. Huang, J. M. Friedman, R. L. Nagel, and G. V. Vidugirus. 1996. Conformational changes in oxyhemoglobin C (Gluβ6$\rightarrow$Lys) detected by spectroscopic probing. *J. Biol. Chem.* 271:372–375.

Hirsch, R. E., C. Raventos-Suarez, J. A. Olson, and R. L. Nagel. 1985. Ligand state of intraerythrocytic circulating HbC crystals in homozygote CC patients. *Blood.* 66:775–777.

Hirsch, R. E., R. E. Samuel, N. A. Fataliev, M. J. Pollack, O. Galkin, P. G. Vekilov, and R. L. Nagel. 2001. Differential pathways in oxy and deoxy HbC aggregation/crystallization. *Proteins.* 42:99–107.

Hofrichter, H. 1986. Kinetics of sickle cell hemoglobin polymerization. III. Nucleation rates determined from stochastic fluctuations in polymerization progress curves. *J. Mol. Biol.* 189:553–571.

Hung, C.-H., M. J. Krasnopoler, and J. L. Katz. 1989. Condensation of a supersaturated vapor. VIII. The homogeneous nucleation of n-nonane. *J. Chem. Physics.* 90:1856–1865.

Hunt, J. A., and V. A. Ingram. 1958. Allelomorphism and the chemical differences of the human hemoglobin A, S, and C. *Nature.* 181: 1062–1065.

Israelachvili, J., and H. Wennerstrom. 1996. Role of hydration and water structure in biological and colloidal interactions. *Nature.* 379:219–225.

Israelachvili, J. N. 1995. Intermolecular and Surface Forces. Academic Press, New York.

Itano, H. A. 1953. Solubilities of naturally occurring mixtures of human hemoglobin. *Arch. Biochem. Biophys.* 47:148–159.

Izmailov, A. F., A. S. Myerson, and S. Arnold. 1999. A statistical understanding of nucleation. *J. Crystal Growth.* 196:234–242.

Kam, Z., and J. Hofrichter. 1986. Quasi-elastic light scattering from soluitons and gels of hemoglobin S. *Biophys. J.* 50:1015–1020.

Kam, Z., H. B. Shore, and G. Feher. 1978. On the crystallization of proteins. *J. Mol. Biol.* 123:539–555.

Koo, E. H., P. T. Lansbury, Jr., and J. W. Kelly. 1999. Amyloid diseases: abnormal protein aggregation in neurodegeneration. *Proc. Natl. Acad. Sci. U.S.A.* 96:9989–9990.

Kuntz, I. D., and A. Zipp. 1977. Water in biological systems. *N. Engl. J. Med.* 297:262–266.

Lauffer, M. A. 1975. Entropy-driven processes in biology. *Mol. Biol. Biophys.* 20:1–264.

Lawrence, C., M. E. Fabry, and R. L. Nagel. 1991. The unique red cell heterogeneity of SC disease: crystal formation, dense reticulocytes, and unusual morphology. *Blood.* 78:2104–2112.

Lessin, L. S., W. N. Jensen, and E. Ponder. 1969. Molecular mechanism of hemolytic anemia in homozygous hemoglobin C disease: electron microscopic study by the freeze-etching technique. *J. Exp. Med.* 130: 443–466.

Lomakin, A., D. S. Chung, G. B. Benedek, D. A. Kirschner, and D. B. Teplow. 1996. On the nucleation and growth of amyloid b-protein fibrils: deterction of nuclei and quatification of rate constants. *Proc. Natl. Acad. Sci. U.S.A.* 93:1125–1129.

Lunelli, L., E. Bucci, and G. Baldini. 1993. Electrostatic Interactions in hemoglobin from light scattering experiments. *Phys. Rev. Lett.* 70: 513–516.

Makinen, M. W., and C. W. Sigountos. 1984. Structural basis and dynamics of the fiber-to-crystal transition of sickle cell hemoglobin. *J. Mol. Biol.* 178:439–476.

Malkin, A. J., and A. McPherson. 1994. Light scattering investigation of the nucleation processes and kinetics of crystallization in macromolecular systems. *Acta Crystallogr. D Crystallogr.* 50:385–395.

McPherson, A., A. J. Malkin, and Y. G. Kuznetsov. 2000. Atomic force microscopy in the study of macroimolecular crystal growth. *Annu. Rev. Biomol. Struct.* 20:361–410.

Minton, A. P. 1977. Non-ideality and the thermodynamics of sickle cell hemoglobin gelation. *J. Mol. Biol.* 110:89–103.

Mutaftschiev, B. 1993. Nucleation theory. *In* Handbook of Crystal Growth (Hurle, D. T. J., editor) Elsevier, Amsterdam. 189–247.

Nagel, R. L., and C. Lawrence. 1991. The distinct pathobiology of SC disease: therapeutic implications. *In* Hematology/Oncology Clinics of North America. (Nagel, R. L., editor) W. B. Saunders, Philadelphia.

Oasawa, Kasi. 1962. A theory of linear and helical aggregation of macromolecules. *J. Mol. Biol.* 4:10–21.

Pennell, R. B. 1974. Composition of normal human red cells. *In* The Red Blood Cell, 2nd ed. (Surgenor, D. M., editor). Academic Press, New York. 93–146.

Perutz, M. F. 1969. The first Sir Hans Krebs lecture: x-ray analysis, structure and function of enzymes. *Eur. J. Biochem.* 8:445–466.

Perutz, M. F. 1976. Structure and mechanism of haemoglobin. *Br. Med. Bull.* 32:195–208.

Petsev, D. N., B. R. Thomas, S.-T. Yau, D. Tsekova, C. Nanev, W. W. Wilson, and P. G. Vekilov. 2001. Temperature-independent solubility and interactions between apoferritin monomers and dimers in solution. *J. Crystal Growth.* 232:21–29.

Petsev, D. N., B. R. Thomas, S.-T. Yau, and P. G. Vekilov. 2000. Interactions and aggregation of apoferritin molecules in solution: effects of added electrolytes. *Biophys. J.* 78:2060–2069.

Petsev, D. N., and P. G. Vekilov. 2000. Evidence for non-DLVO hydration interactions in solutions of the protein apoferritin. *Phys. Rev. Lett.* 84:1339–1342.

Potel, M. J., T. E. Wellems, R. J. Vassar, B. Deer, and R. Josephs. 1984. Macrofiber structure and the dynamics of sickle cell hemoglobin crystallization. *J. Mol. Biol.* 177:819–839.

Prouty, M. S., A. N. Schechter, and V. A. Parsegian. 1985. Chemical potential measurements of deoxyhemoglobin S polymerization. *J. Mol. Biol.* 184:517–528.

Provencher, S. W. 1979. Inverse problems in polymer characterization; direct analysis of polydisperity with photon correlation spectroscopy. *Macromol. Chem.* 180:201–209.

Provencher, S. W. 1982a. A constrained regularization method for inverting data represented by linear algebraic equations. *Comp. Phys. Commun.* 27:213–227.

Provencher, S. W. 1982b. CONTIN: a general purpose constrained regularization program for inverting noisy linear algebraic and integral equations. *Comp. Phys. Commun.* 27:229–242.

Rosenberger, F., S. B. Howard, J. W. Sowers, and T. A. Nyce. 1993. Temperature dependence of protein solubility: determination and application to crystallization in x-ray capillaries. *J. Crystal Growth.* 129: 1–12.

Ross, P. D., R. W. Briehl, and A. P. Minton. 1978. Temperature dependence of nonideality in concentrated solutions of hemoglobin. *Biopolymers.* 17:2285–2288.

Ross, P. D., J. Hofrichter, and W. A. Eaton. 1977. Thermodynamics of gelation of sickle cell deoxyhemoglobin. *J. Mol. Biol.* 115:111–134.

Ross, P. D., and A. P. Minton. 1977a. Analysis of non-ideal behavior in concentrated hemoglobin solutions. *J. Mol. Biol.* 112:437–452.

Ross, P. D., and A. P. Minton. 1977b. Hard quasi-spheroidal model for the viscosity of hemoglobin solutions. *Biochem. Biophys. Res. Commun.* 76:971–976.

Schmitz, K. S. 1990. Dynamic Light Scattering by Macromolecules. Academic Press, New York.

Tammann, G. 1922. Die Aggregatzustaende. Voss, Leipsig.

Tanford, C. 1961. Physical Chemistry of Macromolecules. John Wiley, New York.

Tanford, C. 1980. The Hydrophobic Effect: Formation of Micelles and Biological Membranes. John Wiley, New York.

Tidor, B., and M. Karplus. 1994. The contribution of vibrational entropy to molecular association: the dimerization of insulin. *J. Mol. Biol.* 238: 405–414.

Vasquez, G. B., X. Ji, C. Fronticelli, and G. L. Gilliland. 1998. Human carboxyhemoglobin at 2.2 Å resolution: structure and solvent comparisons of R-state, R2-state and T-state hemoglobins. *Acta. Crystallogr. D Biol. Crystallogr.* 54:355–366.

Voronkov, V. V., and L. N. Rashkovich. 1994. Step kinetics in the presence of mobile adsorbed impurity. *J. Crystal Growth.* 144:107–115.

Williams, R. C. 1973. Concerted formation of the gel of hemoglobin S. *Proc. Natl. Acad. Sci. U.S.A.* 70:1506–1508.

Yau, S.-T., D. N. Petsev, B. R. Thomas, and P. G. Vekilov. 2000a. Molecular-level thermodynamic and kinetic parameters for the self-assembly of apoferritin molecules into crystals. *J. Mol. Biol.* 303: 667–678.

Yau, S.-T., B. R. Thomas, and P. G. Vekilov. 2000b. Molecular mechanisms of crystallization and defect formation. *Phys. Rev. Lett.* 85: 353–356.

Yau, S.-T., and P. G. Vekilov. 2000. Quasi-planar nucleus structure in apoferritin crystallization. *Nature.* 406:494–497.

Zimm, B. H. 1948. The scattering of light and the radial distribution function of high polymer solutions. *J. Chem. Phys.* 6:1093–1099.

Zipp, A., I. D. Kuntz, and T. L. James. 1977. Hemoglobin-water interactions in normal and sickle erythrocytes by protein magnetic resonance tip measurements. *Arch. Biochem. Biophys.* 178:435–441.